communications medicine

Article

https://doi.org/10.1038/s43856-025-00745-6

Host factor PLAC8 is required for pancreas infection by SARS-CoV-2

Lesly Ibargüen-González[1,14], Sandra Heller[2,14], Darío López-García[3], Hanna Dietenberger[4], Thomas FE Barth[4], Patricia Gallego[5], Israel Fernández-Cadenas[6], Sayoa Alzate-Piñol[6], Catalina Crespí[5,7], Julieth A. Mena-Guerrero[1], Eugenia Cisneros-Barroso[7,8], Alejandro P. Ugalde[9], Gabriel Bretones[9], Charlotte Steenblock[10], Alexander Kleger[2,11], Marta L. DeDiego[3] ✉ & Carles Barceló[1,12,13] ✉

Abstract

Background Although COVID-19 initially caused great concern about respiratory symptoms, mounting evidence shows that also the pancreas is productively infected by SARS-CoV-2. However, the severity of pancreatic SARS-CoV-2 infection and its pathophysiology is still under debate. Here, we investigate the consequences of SARS-CoV-2 pancreatic infection and the role of the host factor Placenta-associated protein (PLAC8).

Methods We analyze plasma levels of pancreatic enzymes and inflammatory markers in a retrospective cohort study of 120 COVID-19 patients distributed in 3 severity-stratified groups. We study the expression of SARS-CoV-2 and PLAC8 in the pancreas of deceased COVID-19 patients as well as in non-infected donors. We perform pseudovirus infection experiments in PLAC8 knock-out PDAC and human beta cell-derived cell lines and validate results with SARS-CoV-2 virus.

Results We find that analysis of circulating pancreatic enzymes aid the stratification of patients according to COVID-19 severity and predicts outcomes. Interestingly, we find an association between PLAC8 expression and SARS-CoV-2 infection in postmortem analysis of COVID-19 patients both in the pancreas and in other bonafide SARS-CoV-2 target tissues. Functional experiments demonstrate the requirement of PLAC8 in SARS-CoV-2 pancreatic productive infection by pseudovirus and full SARS-CoV-2 infectious virus inoculum from Wuhan-1 and BA.1 strains. Finally, we observe an overlap between PLAC8 and SARS-CoV-2 immunoreactivities in the pancreas of deceased patients.

Conclusions Our data indicate the human pancreas as a SARS-CoV-2 target with plausible signs of injury and demonstrate that the host factor PLAC8 is required for SARS-CoV-2 pancreatic infection, thus defining new target opportunities for COVID-19-associated pancreatic pathogenesis.

Plain language summary

SARS-CoV-2 virus can be found in the pancreas following infection. We investigated whether the pancreas is damaged by the infection and whether there are changes of the pancreatic enzymes that the pancreas produces and circulates around the rest of the body. A particular protein called the placenta-associated protein 8 (PLAC8) expression was found in people who died following SARS-CoV-2 infection. We show this protein is required for SARS-CoV-2 pancreatic infection and viral replication. PLAC8 could be further investigated as a target for drugs to treat COVID-19 that could reduce the impact on the pancreas.

COVID-19, the respiratory disease caused by SARS-CoV-2, has been associated with a wide range of symptoms and complications, affecting not only the lung but also other organs in the body including the gastrointestinal system[1,2]. Among the less studied, but potentially occurring with severe complications, is the infection of the pancreas, a gland responsible for producing hormones like insulin and digestive enzymes. While the exact mechanism of how SARS-CoV-2 affects the pancreas is not yet fully understood, several studies reported pancreatic inflammation, injury, and dysfunction in some COVID-19 patients[3–8]. Taken together, this raises concerns about the potential long-term impact on pancreatic function and the overall metabolic health of those affected.

Placenta-associated 8 (PLAC8) is a highly conserved protein that is expressed in various tissues like the placenta as well as the respiratory system or the gastrointestinal tract[9]. PLAC8 has been implicated in the regulation of multiple cellular processes like autophagy or cell motility[10]. Previous studies have suggested that PLAC8 also plays a prominent role in pancreatic

A full list of affiliations appears at the end of the paper. ✉e-mail: marta.lopez@cnb.csic.es; carles.barcelo@gmail.com; CBarcelo@umanresa.cat

neoplastic transformation[11–13]. Furthermore, PLAC8 has recently been identified as an essential host factor for SARS-CoV-2 infection in human lung cancer cell lines[14] and for swine acute diarrhea syndrome coronavirus (SADS-CoV) in a swine primary intestinal epithelial culture[15] supporting a potential role of PLAC8 as a pan-CoV infection factor.

In this work, we investigated the impact of SARS-CoV-2 infection on the pancreas as well as the potential relationship with PLAC8. Our data confirm previous studies reporting morphological changes associated with SARS-CoV-2 viral infiltration in the autopsy of the pancreas of patients who died from COVID-19. Notably, the quantification of circulating pancreatic lipase contributed to the stratification of patients according to COVID-19 severity. Interestingly, PLAC8 overexpression was associated with SARS-CoV-2 infection by postmortem analysis of COVID-19 patients in independent series both in the pancreas and in previously described SARS-CoV-2 target organs. Functional studies employing pancreatic cancer cell lines and a beta cell-derived model revealed the requirement of PLAC8 for an efficacious infection of the pancreas. Finally, we observed an overlap in PLAC8 and SARS-CoV-2 immunoreactivity in the islets of deceased patients. In conclusion, our data confirm the human pancreas as a SARS-CoV-2 target and demonstrate that host factor PLAC8 is required for SARS-CoV-2 pancreatic infection defining new target opportunities for COVID-19-associated pancreatic pathogenesis.

Methods

Patients and samples

Patient tissue for immunohistochemical analysis. Sections of human tissue were provided by the pathology department of Ulm University. A board-certified pathologist (Thomas F.E. Barth) approved non-neoplastic tissue integrity. All experiments were executed according to the guidelines of the Ethics Committee of the Federal General Medical Council and approved by the Ethics Committee of the University of Ulm (vote for usage of archived human material 03/2014 and is in compliance with the ethical principles of the Declaration of Helsinki.. Due to retrospective analysis of long-term archived biomaterial, specific informed consent was waived by the Ethics Committee of the University of Ulm.

Patient tissue for immunofluorescence and immunohistochemistry analysis. Autoptic material was retrieved from twelve patients who died of COVID-19 in 2020-21 and from five control patients who died of other causes. Pancreatic tissue was fixed in formalin and embedded in paraffin. The autopsies were performed at the Institute of Pathology at Universitätsklinikum Carl Gustav Carus in Dresden, Germany, or the Institute of Pathology at Universität Regensburg, Germany. Tissue samples were received from the pathology institutes with the respective approval of local ethics committees and collected in the frame of the German Registry for COVID-19 Autopsies (DeRegCOVID). Written informed consent to perform autopsies and to use the tissues for research purposes was obtained from patient relatives. Normal pancreatic tissues were obtained from Zyagen. All Zyagen human tissues-derived products are made of tissues obtained from certified tissue banks in the USA with informed consent given by donors so that their tissues could be included in any biomedical study in compliance with the ethical principles of the Declaration of Helsinki. Main relevant clinical features (Supplementary Table S1).

Samples for blood analysis. We performed a retrospective cohort study from a total of 80 subjects with COVID-19 who had a positive SARS-CoV-2 RT-PCR for whom blood samples were taken within 48 h of hospital admission between August 7th, 2020 and June 17th, 2021 from the Biobank Unit located in the Hospital Universitari Son Espases (HUSE) or COVID19-negative healthy volunteers from the Blood and Tissue Bank of the Balearic Islands in the same period. Informed consent was given by donors so that their samples could be included in any derived biomedical study. This study was conducted in agreement with the Good Clinical Practice principles and the Declaration of Helsinki for ethical research. Ethical approval for this project (IB 4172-20 PI, 26 May 2020) was obtained from the ethics committee of the Balearic Islands and waived the requirement for informed consent, due to the emergency situation.

Mendelian randomization analysis. Data was obtained either from DECODE GENETICS (available at www.decode.com/summarydata/) or from Covid-19 Host Genetics Consortium (available at https://www.covid19hg.org) which are public available databases. Both databases based its research on the participation of individuals who have provided biosamples and their informed consent to use to research human genetics.

Pseudovirus experiments

Plasmids. The plasmids pLenti-CRISPRv2-PLAC8-sg1 (KO1), -sg2 (KO2), used to generate PLAC8 KO cells, and the plasmid encoding a nontargeting control -NT sgRNA, were kindly donated by Prof. Carlos López-Otín[14].

For pseudotyping lentiviral particles, pcDNA3.1 plasmids encoding for Spike SARS-CoV2 Wuhan-1, BA.1, and BA4/5 variants-of-concern (VOCs) were obtained from Dr. Thomas Peacock (Barclay lab, Imperial College London, UK). psPAX2 was a gift from Dr. Didier Trono (Addgene plasmid #12260); pLV-mCherry encoding the reporter protein mCherry was a gift from Dr. Pantelis Tsoulfas (Addgene plasmid #36084); pcDNA3 mCherry was a gift from Dr. Scott Gradia (Addgene plasmid #30125); pcDNA3.1(+) eGFP was a gift from Dr. Jeremy Wilusz (Addgene plasmid #129020).

Generation of pseudotyped lentivirus models. Pseudotyped lentiviruses were generated as previously described[14,16]. Briefly, to generate SARS-CoV-2 pseudoviruses, human embryonic kidney 293 (HEK 293, ATCC® CRL-1573™) cells were seeded in a 10 cm^2 plate at 4.5×10^6 cells/plate, in DMEM (ThermoFisher Scientific, #11995073) supplemented with 10% fetal bovine serum (FBS) and 1x Normocin (Invivogen, #ant-nr1) and grown overnight at 37 °C, 85% relative humidity, 5% CO_2. Next day, HEK 293 cells were then cotransfected with 15 µg of psPAX2: pcDNA3.1Spike VOC: pLV-mCherry at a ratio 1:1:1 (i.e. 5:5:5 µg) using Lipofectamin™ 3000 transfection reagent (ThermoFisher Scientific, #L3000015). Pseudoviruses harvested from the supernatant at 48 h to

72 h post-transfection were filtered (0.44 µm, Millipore Sigma, #SLHA033SS) and concentrated with 50kDa-PES (ThermoFisher Scientific, #88540) during 20 min at 14,000 g RT and stored at −80 °C.

Cell culture. The cell lines HPAF-II, MIA PaCa-2, and SUIT-2 were provided by Dr. Marcos Malumbres (CNIO, Spain). 1.4E7 cell line was provided by Dr. Alexander Kleger (Ulm University, Germany). African green monkey kidney epithelial Vero E6 cells were kindly provided by Prof. Luis Enjuanes (Centro Nacional de Biotecnología, CNB-CSIC, Spain). HPAF-II, MIA PaCa-2, SUIT-2, and 1.4E7 cell lines were cultured in RPMI-1640 medium (Roswell Park Memorial Institute; Gibco), while HEK-293T and Vero E6 cells were cultured in DMEM medium (Dulbecco's Modified Eagle Medium; Gibco). Both media were supplemented with 10% Fetal Bovine Serum (FBS) (v/v) (Gibco), 100 µg/ml of normocin (Invitrogen), 1 M HEPES (Gibco) and 1 % (v/v) of GlutaMax (Gibco). The cells were kept in an incubator at 37°C in a humid atmosphere with 5% CO_2. Periodic passages were made using DPBS 1X (Dulbecco's Phosphate Buffered Saline; Gibco) to wash the cells and TrypLE™ Express 1X (Gibco) or EDTA-trypsin (Gibco) to recover them, since all the cell lines were attached and grew in monolayer. Tests were performed to detect contamination by *Mycoplasma sp*. by PCR every other week.

Lentivirus production for the generation of KO cells. To make a Knock-out (KO) cell, lentiviruses were produced with the different vectors of interest, following the recommendations of Invitrogen. 6×10^6 HEK-293T cells were seeded in 10 cm plates (Sarstedt). The cells were transfected with 6 µg of psPAX2, 3.3 µg of 4 pMD2.G, and 7.7 µg of the

corresponding pLenti plasmid (ratio 1.8:1:2.3 respectively), using Lipofectamine 3000 (Invitrogen). The following pLenti were used: pLenti-CMV-ZSGreen-P2AHygro as selection control, pLentiCRISPR v2 NT_0569 as a vacuum vector, and two pLentiRISPR v2 of two guides (sg1 and sg2) of PLAC8 for the realization of KO. After 6 h of incubation, the medium was replaced by Opti-MEM (Gibco) supplemented with GlutaMAX 1X, 1 mM sodium pyruvate (Gibco), and 5% FBS. At 24 h and 52 h post-transfection, viral supernatants were collected, filtered through a 0.45 µm filter, and concentrated with Pierce™ Protein Concentrator PES 50 K MWC0 (ThermoFisher Scientific) at 14,000 *g* at room temperature up to 2 ml per plate. Finally, they were stored at -80°C until use.

Generation of PLAC8 KO cell lines. To generate a stable PLAC8 knockout, 8×10^5 cells per well were seeded in 24-well plates. The next day, infections with lentiviruses containing pLenti-CRISPRv2-PLAC8-sg1 (KO1), -sg2 (KO2) and nontargeting control (NT) were performed using 200 µL of a 1:1 mixture of concentrated virus and media viral supernatants. At 48 h post-infection the selective medium was replaced with supplemented RPMI plus 2 µg/ml of puromycin. The selection was allowed for 10 days until all cells of a noninfected dish had died. At this point NT, KO1, and KO2 cell lines were pooled and knock-out was analyzed by Western Blot.

Western Blot analysis. To confirm the knock-out of PLAC8, cells were lysed in RIPA buffer containing protease and phosphatase inhibitors cocktail (Thermo Scientific, #78442). Protein concentration was determined using Pierce® BCA Protein Assay Kit (Thermo Scientific). Equal amounts of protein (20–30 µg) were resolved by 8 to 15% SDS PAGE MiniPROTEAN® TGX gels (Bio-Rad), from samples previously prepared with Laemmli Buffer 4X™ (Bio-Rad) supplemented with 5% of β-mercaptoethanol (Sigma) and heated to 98°C for 5 min and transferred to Trans-Blot PVDF Transfer membranes (Bio-Rad, #1704157). Membranes were blocked for 1 h at room temperature with TBST (0.1% Tween 20) containing 10% milk or 5% BSA. Membranes were incubated at 4 °C with primary antibodies diluted in TBS-T containing 10% milk, anti-PLAC8 1:1000 (HPA040465, Sigma), anti-ACE2 1:1000 (SN0754, Invitrogen), anti-Actin Monoclonal 1:1000 (ACTN05, Invitrogen), anti-beta-Actin Polyclonal 1:2,000 (20536-1-AP, Proteintech), anti-Alpha-Tubulin Polyclonal 1:1000 (11224-1-AP, Proteintech), and antiGFP (SAB4301138, Sigma-Aldrich). After washing with TBS-T, the membranes were incubated for 2 h at room temperature with secondary antibodies in TBS-T containing 10% milk: anti-Mouse IgG (HAF018, R&D Systems) and anti-Rabbit IgG (A9196, SigmaAldrich) at 1:2000 and 1:10,000 dilutions, respectively, both conjugated with HRP. Finally, the protein bands were visualized using Clarity™ Western Blot ECL (Bio-Rad) and recorded with ImageQuant LAS4000 (Fujifilm).

SARS-CoV-2 infection assays

Viruses and virus titrations. Virus stocks of SARS-CoV-2, Wuhan-1 and BA.1 strains, were grown in Vero E6 cells, respectively, under BSL3 conditions. Both strains (kindly provided by L. Enjuanes, CNB-CSIC) were isolated in Vero E6 cells starting from nasopharyngeal swabs from patients with COVID-19 from Hospital 12 de Octubre, Madrid, Spain[17].

SARS-CoV-2 virus titrations were performed in Vero E6 cells grown in 24-well plates and infected with ten-fold serial dilutions of the virus, as previously described[18]. After 1 h absorption, cells were overlaid with low electroendosmosis agarose (Pronadisa) and incubated for 3 days at 37 °C. For all virus titrations, cells were fixed with 10% formaldehyde in phosphate buffer saline (PBS) and permeabilized with 20% methanol. Viral plaques were visualized and counted using crystal violet staining.

Immunofluorescence microscopy and flow cytometry. Confluent monolayers of human SUIT-2 cells grown on sterile glass coverslips (24-well plate format) were mock-infected or infected (MOI 1) with SARS-CoV-2 (Wuhan-1 and BA.1 strains). At 24 hours postinfection (HPI), the cells were fixed and permeabilized with 10% formaldehyde and 0.1%

Triton X100 for 20 min at room temperature. Then, cells were blocked with 2.5% BSA in PBS and SARS-CoV-2 nucleocapsid (N) protein was detected with a rabbit anti-N antibody at 1:1000 dilution (Genetex GTX135357). Coverslips were washed with PBS for 4 times, and incubated with secondary anti-rabbit Ab conjugated to Alexa Fluor 488 (Invitrogen), for 45 min at room temperature. Nuclei were stained using DAPI (ThermoFisher Scientific). Coverslips were analyzed on a Leica DMi8 S widefield epifluorescence microscope. Images were acquired with the same instrument settings and analyzed using the Fiji software. To calculate the percentage of infection, more than 600 cells per condition were counted.

Alternatively, confluent monolayers of human SUIT-2 cells grown on sterile glass coverslips (6-well plate format) were mock-infected or infected (MOI 1) with SARS-CoV2 (Wuhan-1 and BA.1 strains). At 24 hours post-infection (hpi), the cells were detached from the wells, and the pelleted cells were fixed and permeabilized with 10% formaldehyde and 0.1% saponin for 20 min at room temperature. Then, cells were blocked with 10% FBS in PBS and SARS-CoV-2 nucleocapsid (N) protein was detected with a rabbit anti-N antibody (Genetex GTX135357). Cells were washed with PBS and 0.1% saponin for 4 times, and incubated with secondary anti-rabbit Ab conjugated to Alexa Fluor 488 (Invitrogen), during 45 min at room temperature. The cells were analyzed in a FACSAria Fusion (Becton Dickinson), and the percentage of infected cells was determined using the FlowJo software (TreeStar).

Blood analysis

Patients. Three patient subgroups of 40 sex and age-matched patients from a retrospective study were defined using the WHO ordinal scale of clinical improvement (OSCI) as described[19]: 40 control cases (WHO OSCI = 0), 40 patients with severe COVID-19 (WHO OSCI = 3–4) admitted to the Ward, and 40 patients with critical COVID-19 (WHO OSCI = 5–8) admitted to the ICU. Our control group comprised 40 healthy uninfected subjects (Healthy), matched by age and sex.

Plasma samples measurements. Plasma samples were collected in two 10-ml EDTA and a 4.5-ml tube with sodium citrate and centrifuged at 2000 × *g* for 10 min as previously described (Durat et al., 2014) and fractionated by automation (Janus robotic liquid handlers; PerkinElmer). Typically, 6–8 h elapsed between sample collection and freezing.

Clinical data were collected during the patient standard of care and final discharge diagnosis. Measurements of C-Reactive protein (CRP), and D-Dimer, Lipase and Protease plasma concentrations were determined at Hospital Son Espases Facilities through the hospital automation system by Alinity I (AbbottDiagnostics).

Immunofluorescence analysis

Immunofluorescence. Paraffin sections were deparaffinized in Neo-Clear (Merck) and rehydrated through a descending-graded ethanol series. Antigen retrieval was performed in citrate retrieval buffer pH 6.0, using a Decloaking Chamber NXGEN (Menarini Diagnostics) at 110 °C for 3 mins. Sections were blocked in blocking buffer (PBS containing 1% BSA (w/v), 0.1% (v/v) Triton X-100, 5% (v/v) goat serum) for 1 h at room temperature, followed by incubation with primary antibody diluted in PBS containing 1% BSA (w/v), 5% (v/v) goat serum at 4 °C overnight. Slides were washed in PBS and incubated with appropriate fluorophore-conjugated secondary antibodies in PBS for 2 h at room temperature. Slides were washed in PBS and nuclei were stained with DAPI(Thermo Fisher Scientific) and mounted with an aqueous mounting medium (Aqua-Poly/Mount; Polysciences).

SARS-CoV-2-N antibody validation. For immunofluorescence stainings of SARS-CoV-2 in pancreatic tissue, a mouse monoclonal antibody against the SARS-CoV-2 nucleocapsid protein (SARS-CoV-2-N, Sino Biological, 40143-MM05) was used. This antibody was validated using

negative control pancreatic tissue and lung tissue from a COVID-19 patient that was previously shown to be positive for both the SARS-CoV-2 spike 1 and the nucleocapsid 2 protein. In lung tissue from a COVID-19 patient, many infected cells were detected with some background fluorescence (Fig. S2A). In pancreatic negative control tissue (non-COVID-19), there was no signal, whereas the antibody exhibited a clearly positive signal in tissues from COVID-19 patients (Fig. S2B). Therefore, this antibody was used for all immunofluorescence stainings.

Confocal laser scanning microscopy and fluorescence microscopy. Confocal imaging was performed with a Zeiss LSM 880 inverted confocal laser scanning microscope and ZEN 2010 software (Zeiss). Image processing and analysis were carried out using ImageJ version 1.53q software. The mean fluorescence was measured using ImageJ.

Immunohistochemical analysis

PLAC8 and Spike staining. Tissue sections were deparaffinized, rehydrated and subjected to heat-mediated antigen retrieval in citrate buffer, pH 6. After blocking of endogenous peroxidases (3% H_2O_2) and unspecific antibody binding (2% BSA + 5% serum) PLAC8 antibody (HPA040465, Sigma, 1:100) or SARS-CoV-2 Spike Glycoprotein S1 antibody (GTX632604, Biozol, 1:500) where incubated overnight at 4 °C. Detection was performed by VECTASTAIN® Elite® ABC-HRP and NovaRED® Substrate (Vector laboratories).

SARS-CoV-2 Spike Glycoprotein S1 antibody validation. The specificity of the antibody SARS-CoV-2 Spike GTX632604 (Biozol) was verified in mock and SARS-CoV-2 infected intestinal organoids (2 days postinfection) prepared according to https://doi.org/10.1016/j.jcmgh.2020.11.003. Moreover, staining of consecutive sections of patient-derived SARS-CoV-2 infected colon tissue with two different antibodies (SARS-CoV-2 Spike GTX632604, Biozol; Anti-SARS-CoV-2 Spike Glycoprotein S1 antibody HL257, Abcam) revealed a similar staining pattern supporting specificity of antibodies.

PLAC8 quantification. Bright-field images were acquired using a Leica DM5500B microscope (Leica) with a Leica DMC5400 camera and Leica Application Suite software.

Measurement of PLAC8 stained area was performed using QuPath Software (Bankhead, P. et al. QuPath: Open source software for digital pathology image analysis[20]. Briefly, NovaRED and hematoxylin stainings have been separated using the color deconvolution method followed by thresholding stained areas and counting of pixels in positive classifications. Additionally, areas without tissue have been excluded by setting a threshold or by manual annotation when necessary. Regions of interest containing Islets of Langerhans and Acini have been annotated manually. Accordingly, PLAC8 positively-stained area per total tissue area or annotated area has been calculated.

Mendelian randomization. Mendelian randomization (MR) is a statistical method that leverages genetic variations, specifically single nucleotide polymorphisms (SNPs), to assess causality[21]. The main MR method was inverse-variance weighted. Also, complementary MR approaches were applied: MR-Egger, weighted median, penalized weighted median, and weighted mode approaches. Statistical analysis was conducted in R using TwoSampleMR (version 0.5.6. Stephen Burgess, Chicago, IL, USA). The methodology followed in this study was in accordance with the latest guidelines for Mendelian randomization studies.

To evaluate these causal effects, we use free access summary statistics data from COVID-19 host genetics consortium (COVID19-hg) Genome Wide Association Studies (GWAS) meta-analyses of three different phenotypes available at https://www.covid19hg.org: very severe respiratory confirmed COVID-19 vs. population, hospitalized COVID-19 vs. population cohorts and COVID-19 vs. population cohorts.

The data included studies of populations of various genetic ancestries, including European, mixed-race Americans, Africans, Middle Eastern, South Asian and East Asian individuals. Severe COVID-19 cases were defined as those individuals who required hospital respiratory care or died from the disease, using 9376 cases and 1,776,645 control individuals in this cohort. Moderate or severe COVID-19 cases were defined as those participants who were hospitalized due to symptoms associated with infection in this cohort using 25,027 cases and 2,836,272 control individuals. Finally, a cohort of all cases with SARS-CoV-2 infection reported regardless of symptoms was used and included 125,584 cases and 2,575,347 control individuals. Controls for all three analyses were selected as genetically matched samples by ancestry with no known SARS-CoV-2 infection[14,17]. On the other hand, summary statistics for each enzyme used for MR have been obtained from DECODE GENETICS available at www.decode.com/summarydata/ from the Icelandic Cancer Project using a cohort of almost 40,000 patients and a control population, randomly selected from the National Registry[22].

Significantly associated (p-value $< 5 \times 10^{-8}$) single nucleotide polymorphisms (SNPs) for each enzyme were used as instruments for MR analysis and then performed a clumping of the variants with a threshold of $r2 < 0.001$ using the 1000 G European reference panel. For the significant and robust results, we performed scatterplots and leave-one-out tests that are shown in forest plots. A significant causal association was considered to exist when the p-value was lower than 0.05, complementary methods showed the same direction of the association, and no pleiotropy or heterogeneity was detected.

Statistical analysis. Statistical analysis was performed using GraphPad Prism version 9.0.0 (GraphPad Software, San Diego, CA, USA). Statistical significance was determined using an unpaired two-tailed Student's t-test for comparison of two means. The significance was defined as: *ns (not significant)* $P > 0.05$; *$P < 0.05$; ** $P < 0.01$; *** $P < 0.001$; **** $P < 0.0001$.

Reporting summary

Further information on research design is available in the Nature Portfolio Reporting Summary linked to this article.

Results

Pancreatic damage is associated with COVID-19 severity

Given the rather open debate about the magnitude of COVID-19 impact on pancreatic tissue[5–8], we sought to investigate the damages inflicted by the SARS-CoV-2 virus in the infected patients featuring different degrees of disease severity.

First, we studied postmortem material from patients who died from COVID-19. We stained sections for viral SARS-CoV-2 Spike protein, previously validated for immunohistochemistry in colon sections of a deceased COVID-19 patient and SARSCoV-2 infected intestinal organoids (Fig. S1). In accordance with previous studies[5,6], pancreatic histopathology revealed the presence of SARS-CoV-2 Spike protein in islets and epithelium of the acini. We further validated these findings by immunofluorescence analysis of SARS-CoV-2 nucleocapsid (Fig. S2). This indicates a persistent productive infection during severe COVID-19 (Fig. 1a).

As previously described[5], the morphology of some of the infected cells did not resemble ductal, acinar, or endocrine architecture, indicating a certain degree of tissue hyperplasticity occurring after infection (e.g. shrinkage of the islets, degeneration, and polyploidy of the β-cells were observed). In some patients, mild lymphocytic infiltration of both the endocrine and exocrine pancreas was demonstrated (Fig. S3).

To complement these findings, we analyzed signs of pancreatic injury by measuring plasma levels of pancreatic injury-related enzymes. To this end, we studied plasma in a retrospective cohort study of 120 patients classified into three severity-stratified groups according to the WHO ordinal scale of clinical improvement (OSCI)[19]: 40 control cases (WHO OSCI = 0),

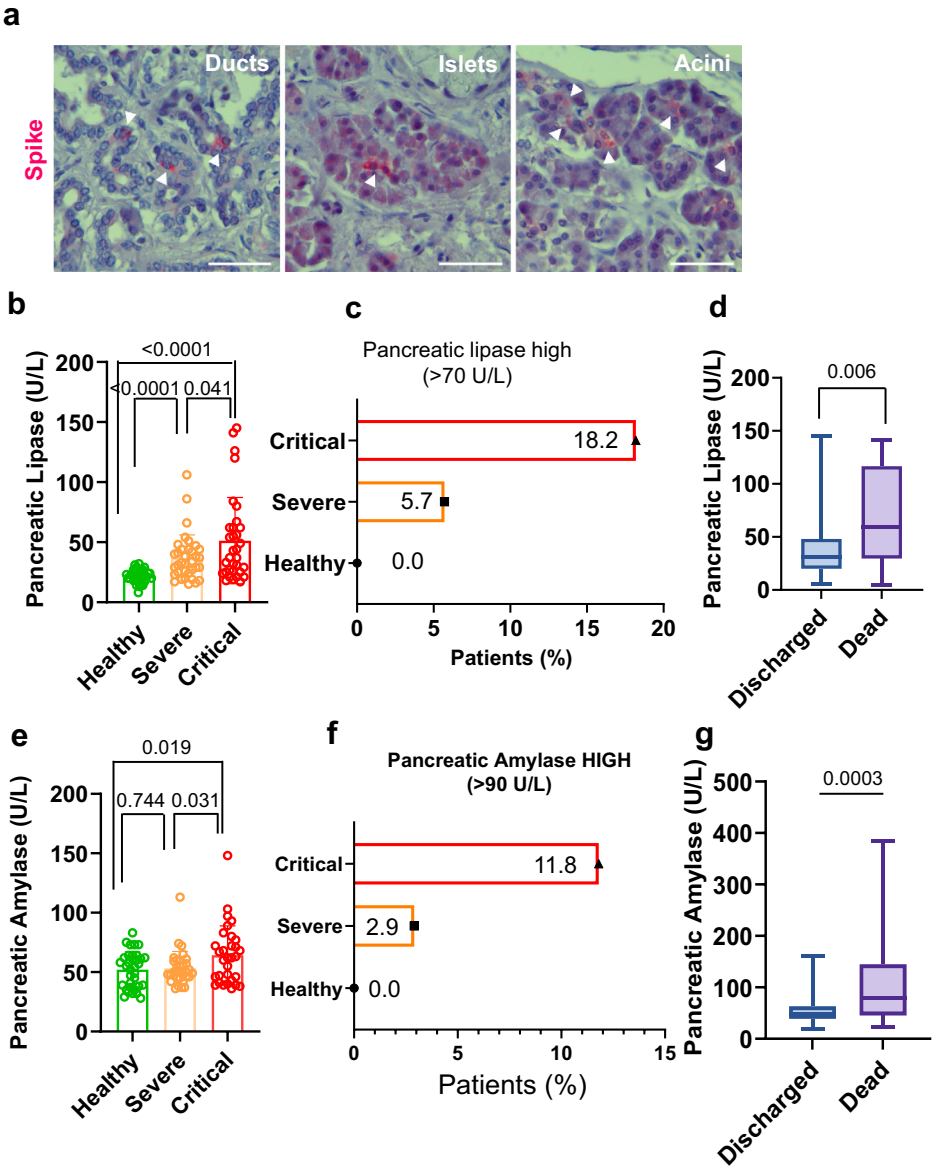

Fig. 1 | SARS-CoV-2 pancreatic infection is associated with damage. a Viral infiltration occurs in both endocrine (Islets) and exocrine pancreas (Ducts and Acini). Sections are stained with anti-SARS-CoV-2 Spike Glycoprotein S1 (Spike, red) and counterstained with Hematoxylin. Bar, 100 μm; **b** Plasma levels of pancreatic injury biomarker pancreatic lipase stratify COVID-19 patients according to severity; **c** Patients (%) with pancreatic lipase above normal blood levels (>70 U/L); **d** Plasmatic levels of pancreatic lipase in hospitalized patients that ultimately were discharged or who died; **e** Plasma levels of pancreatic injury biomarker pancreatic amylase stratify COVID-19 patients according to severity; **f** Patients (%) with circulating pancreatic amylase above normal blood levels (>90 U/L); **g** Plasmatic levels of pancreatic amylase in hospitalized patients that ultimately were discharged or who died. $N = 40$ healthy donors; 40 severe patients; 40 critical patients. Data are presented as mean ± s.e.m. Statistical significance was calculated by ordinary two-tailed unmatched t-test.

40 patients with severe COVID-19 (WHO OSCI = 3–4), and 40 patients with critical COVID-19 (WHO OSCI = 5–8).

Demographic and clinical characteristics of the three groups were stratified according to their severity assignments by the clinical care team at Hospital Son Espases (HUSE), Palma, Spain (Table 1). The study cohort comprised 47% females and featured an average age of 61.7 years. The most frequent co-morbidities were dyslipidemia (43.3%), obesity (30%), and hypertension (26.7%). Severe and critical severity groups were very similar for most characteristics and the control group exhibited significant differences with respect to Total ($p = 0.015$) in Age (56 vs. 61.7 y, $p < 0.0001$), Hypertension (10% vs 26.7%, $p = 0.012$), Type-2 Diabetes Mellitus (T2DM) (2.5% vs 19.3%, $p = 0.0039$) and Chronic Obstructive Pulmonary Disease (COPD) (0% vs 9.2%, $p = 0.0031$) (Table 1).

Elevated blood levels of pancreatic enzymes such as lipase and amylase are typically documented during pancreatic injury[3,4,23]. Given its rather long-lasting elevated levels, pancreatic lipase plasma levels not only render as the favored circulating diagnostic biomarker for pancreatic injury in terms of sensitivity and diagnostic window but is also a useful diagnostic biomarker in the early and late stages of pancreatitis[24–26].

In our experimental setting, pancreatic lipase plasma levels aided in significantly stratify patients according to the severity in three groups (healthy vs severe and healthy vs critical, $p < 0.0001$; severe vs critical, $p = 0.041$) (Fig. 1b). Significant discrimination between the critical and severe groups was also achieved upon measuring pancreatic amylase, a less specific biomarker for pancreatic damage (Fig. 1e). Moreover, plasma levels of both pancreatic enzymes, indicative of pancreatic damage, exhibited a significant correlation between themselves ($r = 0.46$, $p < 0.0001$) (Fig. S4a).

The normal blood levels of amylase and lipase are 0–90 U/L and 0–70 U/L, respectively[23,27]. Interestingly, the number of patients classified according to the levels of these enzymes in moderate or elevated, mirrored the magnitude of COVID-19 disease. Patients with higher pancreatic lipase blood levels than baseline (hyperlipasemia) showed a 3-fold increase (Fig. 1c) while patients with higher amylase levels exhibited a 4-fold increase (Fig. 1f) when comparing critical vs severe COVID-19 patients. None of the healthy donors exhibited an increase of these enzymes (Fig. 1c, f) Notably, the differentiation of severity groups related to circulating pancreatic enzymes resembled the distribution of the inflammatory markers C-reactive protein (CRP) and DDimer that are hallmarks of severe COVID-19 (Fig. S4b, d). Moreover, the Pearson correlation demonstrated that levels of plasma pancreatic lipase significantly correlated with these two typically used clinical variables that discriminate severity-stratified groups, CRP ($r = 0.27$ $p = 0.018$) and D-Dimer ($r = 0.47$ $p = 0.004$) (Fig. S4c, e).

Table 1 | Baseline characteristics of the sample population

	Total (n = 120)	Control group (n = 40)	Severe COVID19 (n = 40)	Critical COVID19 (n = 40)	p-value
Age (years)	61.7	56	66.3	62.8	<0.0001*
Sex					0.1753
Female	56 (47%)	22 (55%)	20 (50%)	14 (35%)	
Male	64 (53%)	18 (45%)	20 (50%)	26 (65%)	
Comorbidities					
Chronic pancreatitis	1 (0.83%)	0 (0%)	0 (0%)	1 (2.5%)	0.1308
Hypertension	32 (26.7%)	4 (10%)	13 (32.5%)	15 (37.5%)	0.0124
Type 2 DM	23 (19.3%)	1 (2.5%)	10 (25%)	12 (30%)	0.0039
Obesity	36 (30%)	7 (17.5%)	17 (42.5%)	12 (30%)	0.0510
COPD	11 (9.2%)	0 (0%)	4 (10%)	7 (17.5%)	0.0031
Dyslipidemia	52 (43.3%)	9 (22.5%)	23 (57.5%)	20 (50%)	0.0040
Smokers	18 (15%)	3 (7.5%)	5 (12.5%)	10 (25%)	0.0782

Data are presented as the mean (age), absolute numbers and percentage (%). * One-way ANOVA was used to calculate the P-value. All values except for "Age" are calculated with the Chi-square test.

We then tested the potential ability of pancreatic lipase and amylase plasma levels in discriminating between patients who ultimately were discharged or who died in hospitalized centers. We found that both, plasmatic pancreatic lipase and amylase represent parameters that can reliably be used to significantly discriminate between these two groups (Pancreatic lipase, $p = 0.006$; Amylase, $p = 0.0003$) (Fig. 1d, g) further reinforcing the role of pancreatic damage in COVID-19 pathogenesis.

Finally, we used a two-sample Mendelian Randomization (MR) approach[21] to evaluate the causal association between COVID-19 severity and plasma levels of pancreatic amylase and pancreatic lipase. Along the same lines as the other results for pancreatic amylase, those patients with COVID-19 severe or critical symptoms had higher levels of biomarkers of pancreatic damage. We analyzed 8,779 cases with severe or critical COVID-19 symptoms and 1,001,875 controls[28]: odds ratio (OR), 0.95 ([95% CI, 0.91–1.01], standard error (SE) = 0.07, beta=0.1 and p value = 0.03). Although the leave-oneout analysis showed that causality was not driven by a single nucleotide variant, there was no pleiotropy or heterogeneity, and complementary methods showed the same direction of the association **(Fig S5a, b)**. In contrast, no significant associations were observed with the inpatient and COVID-19 vs. population groups and no significant associations were observed with pancreatic lipase enzyme.

PLAC8 is overexpressed in the SARS-CoV-2-infected pancreas

A potential link between SARS-CoV-2 infection and the upregulation of PLAC8 expression in lung epithelial cells has been reported[14]. Since PLAC8 has been described to be prominently expressed in the perturbed pancreas[10–12], we analyzed the association between SARS-CoV-2 infection and PLAC8 distribution in pancreatic tissues from deceased individuals with COVID-19.

We studied the distribution of PLAC8 in the pancreas by immunohistochemical analysis of postmortem material from a patient described in Müller et al. [6] and found that PLAC8 was mainly expressed in islets and to a lesser extent in acini (Fig. 2a, b; Fig S6). This is consistent with a putative role of PLAC8 during viral infection given the detection of significantly higher levels of this protein in COVID-19 patients ($n = 3$) than in non-infected individuals ($n = 3$) in the whole pancreatic tissue ($p = 0.0135$), acini ($p = 0.0351$) and islets ($p < 0.0001$) (Fig. 2a,b). An independent series from a different center based on $n = 3$ COVID-19 patients and $n = 3$ non-infected controls showed stronger significance for pancreatic tissue ($p < 0.0001$), acini ($p < 0.0001$) and islets ($p < 0.0001$) (Fig S7).

We further substantiated our quantifications by using an independent series of SARS-CoV-2 infected patients ($n = 2$) vs non-infected individuals ($n = 3$) and quantified the expression levels in immunofluorescence stainings. Using this different technique, we obtained similar results for the pancreatic tissue ($p = 0.021$) and islets ($p = 0.0017$) while non-significant differences were documented in acini ($p = 0.167$) (Fig S8).

These results reiterate that PLAC8 could be implicated in pancreatic COVID-19 pathogenesis.

PLAC8 overexpression is associated to SARS-CoV-2 infection across various organs

To clarify the significance of host factor PLAC8 expression in SARS-CoV-2 infection we studied postmortem material from different organs. Since PLAC8 expression is limited to certain organs/tissues, we expanded our study to analyze the tissues previously described as bona-fide SARS-CoV-2 targets[1,2] that exhibit a detectable level of PLAC8 by immunohistochemical analysis i.e. respiratory or gastrointestinal system (https://www.proteinatlas.org/ENSG00000145287-PLAC8/tissue).

Our immunohistochemical analysis showed that PLAC8 protein is significantly overexpressed in deceased individuals infected with SARS-CoV-2 as compared to noninfected donors in the colon ($n = 1$ control; $n = 2$ COVID-19; $p = 0.0005$), liver ($n = 1/1$; $p = 0.0094$) and lung ($n = 5/6$, $p = 0.009$) reinforcing the putative role of PLAC8 in SARS- CoV-2 infection. (Fig S9).

Host factor PLAC8 is required for SARS-CoV-2 pancreatic infection

To further demonstrate the connection between PLAC8 expression and SARS-CoV-2 infection in the pancreas, pancreatic cancer cells featuring PLAC8 knockout (KO) were generated using two different CRISPR sgRNAs (KO1 and KO2) and a non-targeting CRISPR control (NT) as described[14] (Fig. S10a). Genetically modified cells were then subjected to infection with full-length Spike-typed corresponding to different variants of concern (VOC) lentiviruses carrying a mCherry-expressing plasmid. mCherry allows an accurate assessment of infection efficiency by flow cytometry as previously reported[14,16] (Fig S10b). For negative control, the same cell lines were transduced with non-typed lentiviruses carrying a mCherry-expressing plasmid. Knockout of PLAC8 was confirmed by Western blot (Fig. 3a).

Our investigations revealed a significant reduction in infection efficiency in PLAC8 KO cells (KO1 and KO2). Interestingly, the decrease was significant in all tested VOC (Wuhan-1, BA1 and BA4/5). Control experiments performed with non-typed lentiviruses showed almost no detectable infection (Fig. 3a). These findings demonstrate that the loss-of-function of PLAC8 negatively impacts the viral entry of S-typed lentiviruses and therefore a decreased capability of infecting pancreatic cancer cells.

To corroborate our findings in a non-tumoral model recapitulating pancreatic islet SARS-CoV-2 infection, we replicated the same experiments

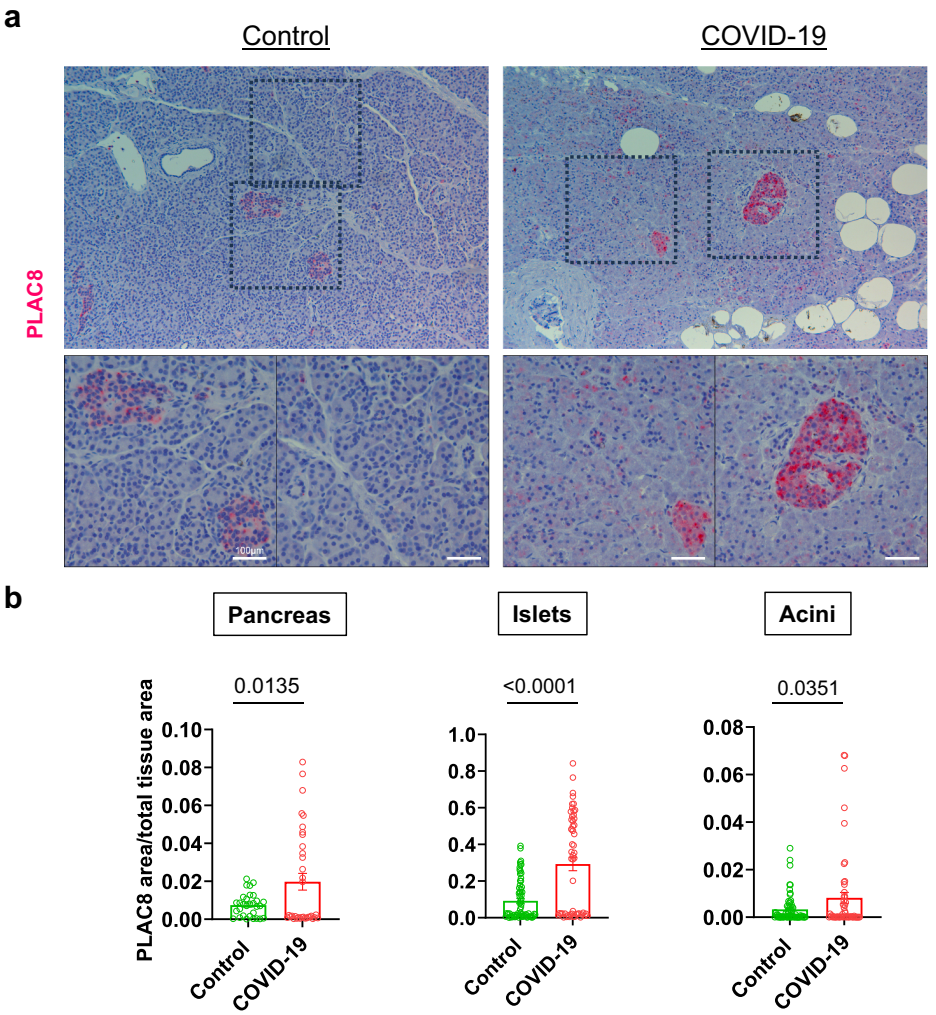

Fig. 2 | Host factor PLAC8 is overexpressed in the pancreas of COVID-19 deceased patients. **a** PLAC8 expression pattern in pancreatic sections of non-infected (Control; $n = 3$) and infected (COVID-19; $n = 3$) deceased patients. Sections are stained for PLAC8 protein (red) and counterstained with Hematoxylin (blue). Rectangles mark areas of higher magnification in the bottom row. Bar, 100 µm; **b** Pancreatic Islets and Acini were manually identified in necropsies and blinded quantified using QuPath. Data are presented as mean ± s.e.m. of PLAC8 positive area relative to the total area for uninfected donors (Control; $n = 2$), and infected patients (COVID-19; $n = 3$). Statistical significance was calculated by ordinary two-tailed unmatched t-test.

with the human islet beta cells-derived model 1.4E7[29]. We generated PLAC8 knock-out using the same CRISPR-based approach and confirmed a similar significant sharp reduction in infection efficiency in all tested VOC upon PLAC8 loss (Fig. S11).

To substantiate these results, we performed rescue experiments by ectopically expressing CRISPR-resistant GFP-fused versions of PLAC8 (GFP-PLAC8) in the CRISPR KO cell lines. Western blot analyses confirmed the knockdown efficacy of endogenous PLAC8 and the overexpression of GFP-fused versions (Fig. 3b). Importantly, infection with S-typed Wuhan-1 lentiviruses indicated that ectopic GFP-PLAC8 is capable of restoring the defects in infection efficiency of the corresponding CRISPR KO cell lines (Fig. 3b). Since previous studies claimed that SARS-CoV-2 pancreatic cell infection was strictly dependent on ACE2[7,30] we analyzed if changes in PLAC8 levels caused by CRISPR-mediated KO or GFP-PLAC8 overexpression impacted the ACE2 receptor. Indeed, Western Blot analysis showed that ACE2 levels remained unaltered upon PLAC8 modulation (Fig. 3b).

These results support the requirement of host factor PLAC8 for an efficient SARS-CoV-2 pancreatic infection.

SARS-CoV-2 productive infection is PLAC8-dependent in a pancreatic cancer cell line

To validate the effect of PLAC8 loss-of-function using full SARS-CoV-2 infectious viruses from Wuhan-1 and BA.1 strains, SUIT-2 PLAC8 NT and KO cell lines were infected with a SARS-CoV-2 inoculum. Viral infection efficacy was assessed by immunofluorescence of the nucleocapsid (N) protein at 24 h postinfection (p.i.). Consistent with our previous results, PLAC8 loss-of-function caused a significant reduction in the number of SARS-CoV-2 infected cells at 24 h p.i. in KO cell for both viral strains (Wuhan-1, $p = 0.0002$; BA.1, $p = 0.0001$) (Fig. 4a).

The viral replication capacity in SUIT-2 PLAC8 NT and KO cell lines was evaluated by analyzing infectious viral titers in the respective cell supernatants. Our results show that an efficient viral replication in the SUIT-2 cell line was significantly impaired by loss-of-function of PLAC8 for both viral strains ($p < 0.0001$) (Fig. 4b).

Host factor PLAC8 co-localizes with SARS-CoV-2 during severe COVID-19

To further confirm PLAC8 requirement for SARS-CoV-2 infection event in pancreatic tissue, expression patterns of PLAC8 and SARS-CoV-2 were analyzed on autopsies from 2 individuals deceased from COVID-19. An archival control (Ctrl #1, non-infected pancreatic tissue collected in 2020) was used to ensure the specificity of SARS-CoV-2 nucleocapsid (N) protein (SARS-CoV-2N) staining. As expected, in this control, the SARS-CoV-2N signal was weak when compared to the SARS-CoV-2N staining in the

COVID-19 patients (Fig. 5a,b). Sections were subjected to the evaluation of not only PLAC8 but also insulin immunoreactivity to define the islet compartment. PLAC8 staining showed a stronger signal in islets as compared to acini in agreement with our previous observations (Fig. 2a).

Morphometric analysis showed that PLAC8 co-localized with SARS-CoV-2N. A robust co-localization was documented especially in the islets, and to a lesser extent in the acinar compartment (Fig. 5b).

Altogether, these experiments point to the requirement of host factor PLAC8 for efficient and productive infection.

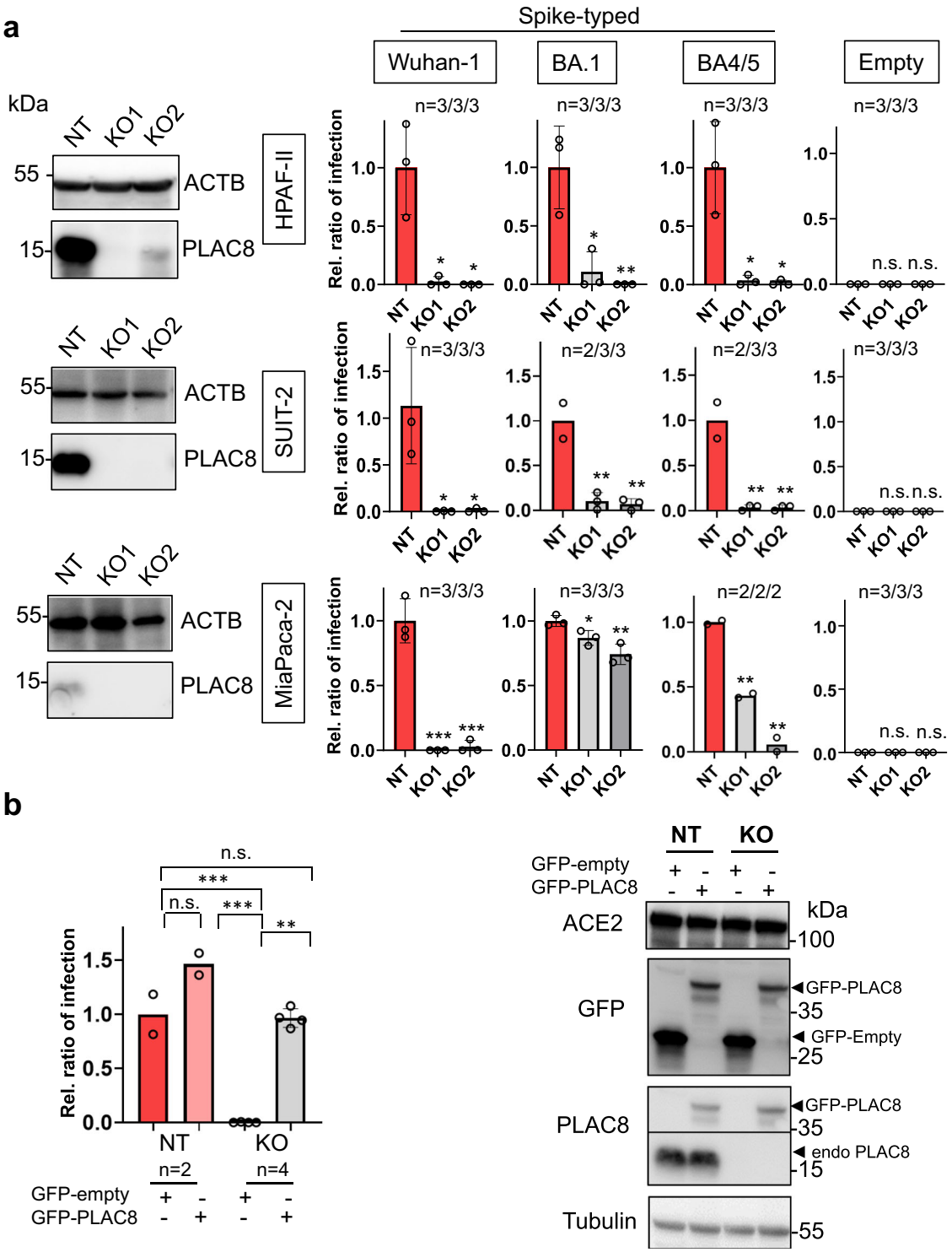

Fig. 3 | Host factor PLAC8 is required for efficient infection by Spike-typed pseudoviruses. a Susceptibility to infection with Spike-typed (corresponding to Wuhan-1, BA.1 or BA4/5 variants-of-concern) or empty vector-typed lentiviruses in exocrine pancreas cell lines MiaPaca-2, HPAF-II and SUIT-2 CRISPR knock-out (KO) cell lines with loss-of-function of PLAC8. NT is a non-targeting CRISPR control. KO was confirmed by Western Blot. Bars represent the average and standard error of the mean (SEM) of the ratio of infected cells in each condition normalized to the non-targeting control cell line NT; **b** Rescue experiments in PLAC8 in SUIT-2 KO cell lines: bar plot showing the average and SEM of the ratio of infection (normalized to NT with GFP-empty vector overexpression) of Wuhan-1 Spike-typed lentivirus in PLAC8-KO1 and KO2 that overexpress CRISPR-resistant GFP-PLAC8 construct. Knock-out and rescue were confirmed by Western Blot. The number of independent biological replicates (n) is indicated. The significance above each bar represents the t-test p-value between indicated conditions. ns, *P*-value ≥ 0.05, **P*-value < 0.05, ***P*-value < 0.01, ****P*-value < 0.001.

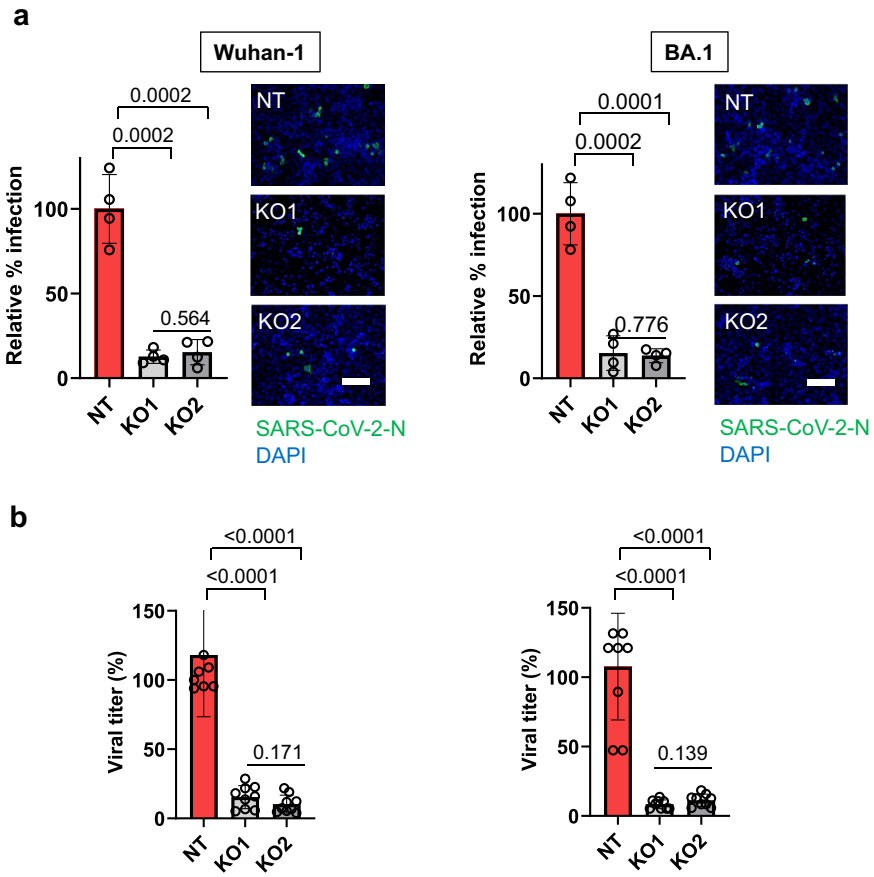

Fig. 4 | SARS-CoV-2 productively infects pancreatic cell lines in a PLAC8-dependent manner. **a** Susceptibility to infection with two strains of full SARS-CoV-2 viruses in SUIT-2 cell line with loss-of-function of PLAC8. Immunofluorescence quantification of the relative number of infected cells at 24 h post-infection in the PLAC8 loss-of-function cell lines relative to CRISPR non-targeting transduced (NT) control cells infected with SARS-CoV-2 ($n = 4$). Right: representative immunofluorescence images of SARS-CoV-2 nucleocapsid protein (green) and cell nuclei (blue) in the indicated cell models. Scale bar, 200 µm; **b** Viral titer count of SARS-CoV-2 in SUIT-2 supernatant at 24 h post-infection. Bars represent the average and SEM of the percentage of infected cells or virus titers relative to CRISPR nontargeting transduced (NT) cells in $n = 3$ biological replicates (three different CRISPR KO cell lines infected independently). The significance above each bar represents the test p-value between each condition and CRISPR non-targeting transduced (NT) cells.

Discussion

Although COVID-19 initially caused great concern about respiratory symptoms, most patients also manifested gastrointestinal symptoms[1,2] and mounting evidence shows that both the endocrine and exocrine pancreas are productively infected by SARS-CoV-2[5,6,8]. However, the prevalence and severity of pancreatic COVID-19 infection, as well as its pathophysiology, are still under debate.

In agreement with previous observations[6,31], IHC analysis from 3 independent series of COVID-19 postmortem specimens revealed a substantial SARS-CoV-2 viral infiltration in both, endocrine and exocrine compartments of pancreatic tissue. Importantly, we could also observe morphological changes indicative of cell damage as previously reported for SARS-CoV-2[5,6] and SARS-CoV[32]. In the previous pneumonia pandemic caused by SARS-CoV infection (2003), the virus was detected not only in the tissues of the lung, liver, kidney, and intestine but also of the pancreas, indicating the pancreas as a potential coronaviral target[33]. Moreover, SARS-CoV infection caused damage of the islets and subsequent acute diabetes[32] suggesting that pancreas is a pan-CoV target with high clinical relevance for potential future CoV pandemics.

Case reports and retrospective cohort studies have revealed an association between pancreatitis-associated hyperlipasemia/hyperamylasemia and COVID-19[3,33]. As SARS-CoV-2 receptors are expressed in the pancreas and endothelial damage can occur, this association is indeed plausible[4]. To interrogate the pancreatic damage inflicted by the SARS-CoV-2 infection, we studied plasma samples from a retrospective cohort comprising 120 patients classified in 3 levels of severity according to the WHO ordinal scale. We found an association between the levels of pancreatic damage biomarker lipase and to a lesser extent the pancreatic amylase in COVID-19 patients according to the severity of infection. Furthermore, these correlated with inflammatory biomarkers typically used in the clinic highlighting a relevant COVID-19-related pancreatic pathogenesis. Blood levels of pancreatic enzymes reflect a balance between the production and clearance of these enzymes. A robust or even a moderate rise in blood levels of lipase and amylase is usually associated with pancreatic injury[23,27]. Here, we report a 3- to 4-fold increase between critical vs severe subgroups in the proportion of patients with elevated plasmatic pancreatic lipase and amylase, respectively. The increased values are associated with histopathological changes and indicate the presence of an injury of the pancreas in COVID-19 patients that might be caused directly by the cytopathic effect triggered by the local SARS-CoV-2 replication. Of note, we cannot dismiss the possibility of an indirect cause for the pancreatic injury such as systemic responses to respiratory failure or the harmful immune response induced by SARS-CoV-2 infection, which also led to damage in multiple organs[34]. Interestingly, our MR study suggests a causal relationship between higher plasma levels of pancreatic amylase and the severity of COVID-19. We identified significantly associated single nucleotide polymorphisms (SNPs) for each enzyme and performed a clustering analysis of these variants. A threshold of $r2 < 0.001$ was applied using the 1000 Genomes Project European reference panel, but a less restrictive threshold of 0.1 could be considered for future studies. Further research is mandatory for the validation and confirmation of these findings in different populations and cohorts, as well as to analyze the link between SARS-CoV-2 infection and up-regulation of PLAC8 expression in lung epithelial cells.

A previous CRISPR-Cas9 screening identified PLAC8 as an essential host factor required for SARS-CoV-2 lung infection[14] and SADS-CoV swine infection[15]. Since a role of PLAC8 has been proposed in pancreatic tumorigenesis[11,12], we investigated the contribution of this protein to the COVID-19-linked pancreatic pathophysiology. Analysis of pancreatic tissue from COVID-19 deceased patients showed substantially elevated PLAC8 levels as compared to uninfected controls ($p = 0.016$) in three independent cohorts. These findings are in line with robust PLAC8 expression documented in lung epithelial cells as demonstrated by single cell

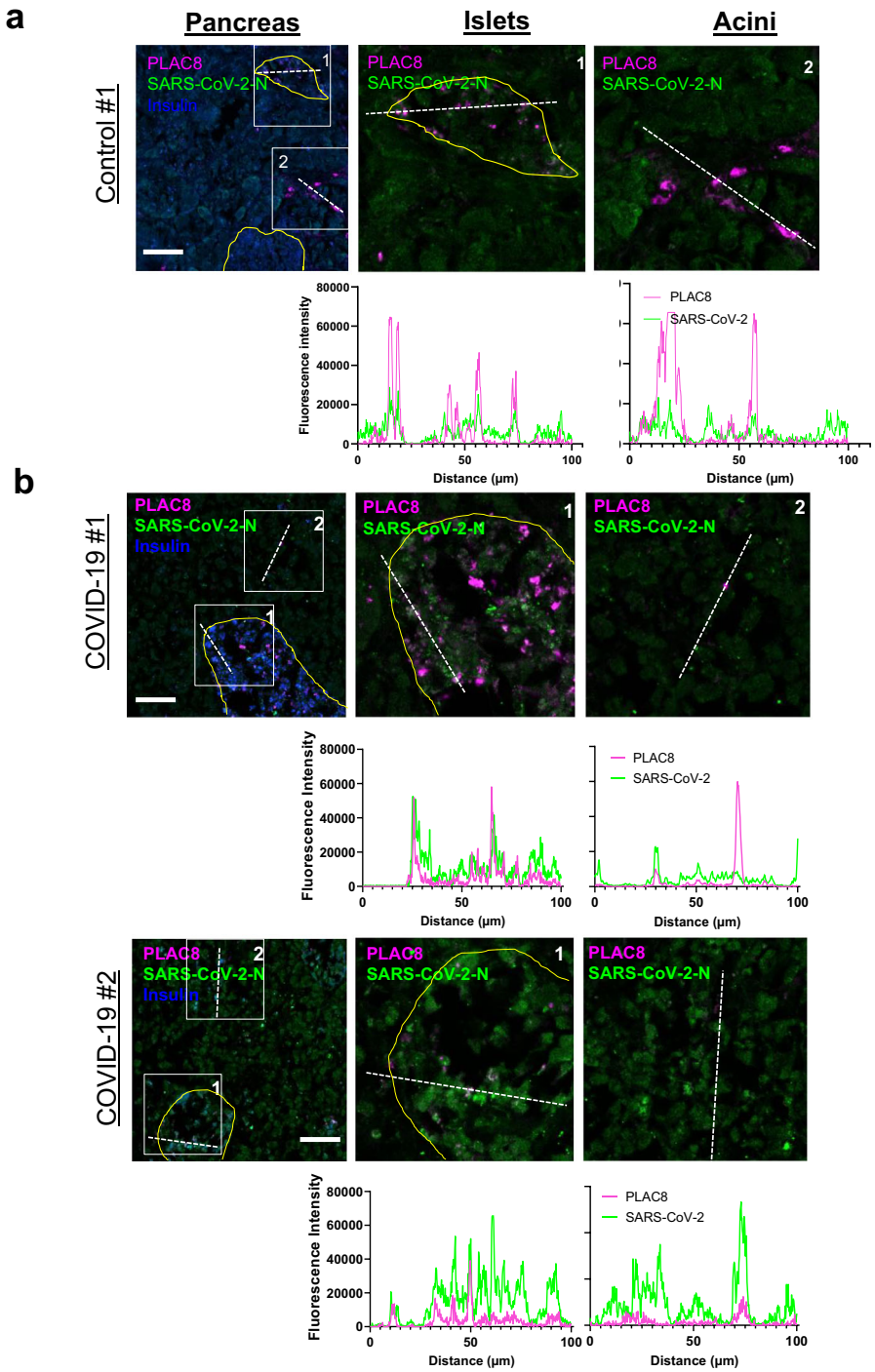

Fig. 5 | Host factor PLAC8 expression correlates with SARS-CoV-2 infection in pancreas of COVID-19 deceased patients. Morphometric analysis of a PLAC8/SARS-CoV-2-N staining of pancreatic tissue from non-infected controls (**a**) and COVID-19 patients (**b**). The fluorescence intensities in the indicated fluorescence channels along the white line were measured. Scale bar, 100 μm.

RNA-seq analysis[14,35–37]. Furthermore, PLAC8 is prominently expressed in the perturbed pancreas, especially in initial events of pancreatic cancer[10–12].

To clarify the significance of host factor PLAC8 expression in SARS-CoV-2 infection we studied postmortem material from different organs. Since PLAC8 expression is limited to certain organs/tissues, we have expanded our study to analyze the tissues previously described as bonafide SARS-CoV-2 targets[1,2] that exhibit a detectable level of PLAC8 by immunohistochemical analysis i.e. respiratory or gastrointestinal system (https://www.proteinatlas.org/ENSG00000145287-PLAC8/tissue).

Our immunohistochemical analysis showed that PLAC8 protein is significantly overexpressed in deceased individuals infected with SARS-CoV-2 in the colon, liver, and lung. Interestingly, this observation agrees with previous RNAseq data analysis[14] and we believe it reinforces the putative role of PLAC8 in SARS-CoV-2 infection.

To study the direct role of PLAC8 in SARS-CoV-2 infection, we generated PLAC8 knockout by two different sgRNA CRISPR/Cas9 in a panel of human pancreatic cancer cell lines. Transduction of KO cells with a Spike-typed pseudovirus comprising Wuhan-1, BA1, and BA4/5 VOC revealed that PLAC8 loss-of-function suppressed to a large extent the infection capability of all SARS-CoV-2 variants. Importantly, these effects were completely restored by ectopically expressing CRISPR-resistant GFP-fused versions of the protein in the KO cell lines.

We replicated our infection experiments in a human pancreatic beta cells-derived model. Although cadaveric islets are in principle the best source for primary beta cells, the quality of islets distributed for research can

be restricted by contamination with nonendocrine cells. Moreover, the purification of beta cells is difficult and not standardized yet. Human islet cells lack proliferation, and therefore, remain viable in culture for a limited period[38]. Thus, replicating our experiments in human islets was not feasible. A model system to study human beta cells is the human cell line 1.4E7 derived by electrofusion of adult human beta cells with the human cell line PANC-1. This cell line retains expression of human beta cell markers such as insulin and insulin secretion can be stimulated by glucose as well as incretin hormone GLP-1, important hallmarks of beta cell function[29]. This cell line proved to recapitulate many aspects of human beta cell physiology.

Therefore, we included this model system in our studies and we further confirmed the effect of PLAC8 loss-of-function using full SARS-CoV-2 infectious virus inoculum from Wuhan-1 and BA.1 strains. Consistently, PLAC8 abrogation resulted in a substantial reduction in the number of infected cells in both KO cell lines tested. Importantly, evaluation of the replicative capacity reflected by infectious viral titers in the respective supernatants showed a decreased efficiency of viral production upon PLAC8 deletion. These results demonstrate for the first time the requirement of PLAC8 for SARS-CoV-2 viral replication in human tissue and are in accordance with previous observations addressing the swine acute diarrhea syndrome coronavirus (SADS-CoV)[15] and SARSCoV-2[14]. This further reinforces our findings and supports the potential of PLAC8 as a pan-CoV therapeutic target.

In conclusion, our data confirm the human pancreas as a SARS-CoV-2 target with plausible signs of injury unveiling the measurement of pancreatic enzymes with prognosis value and demonstrating that host factor PLAC8 is required for SARS-CoV-2 pancreatic infection defining new target opportunities for COVID-19-associated pancreatic pathogenesis.

Data availability

All data supporting the findings of this study are available within the paper and its Supplementary Data. The source data for Figs. 1–5 and Supplementary Figs. S4, 7, 8, 9. 11 can be found in Supplementary Data file. For Mendelian Randomization studies data was obtained either from DECODE GENETICS (available at www.decode.com/summarydata/) or from Covid-19 Host Genetics Consortium (available at https://www.covid19hg.org) which are public (open-access) available databases. Any additional information required to reanalyze the data reported in this paper is available from the lead contact upon request.

Received: 23 October 2023; Accepted: 21 January 2025;
Published online: 03 February 2025

References

1. Moslehi, N. et al. Multi-organ system involvement in coronavirus disease 2019 (COVID-19): A mega review. *J. Fam. Med. Prim. Care* **11**, 5014–5023 (2022).
2. Thakur, V. et al. Multi-organ involvement in COVID-19: Beyond pulmonary manifestations. *J. Clin. Med.* **10**, 446 (2021).
3. Nayar, M. et al. SARS-CoV-2 infection is associated with an increased risk of idiopathic acute pancreatitis but not pancreatic exocrine insufficiency or diabetes: long-term results of the COVIDPAN study. *Gut* **71**, 1444–1447 (2022).
4. de-Madaria, E. & Capurso, G. COVID-19 and acute pancreatitis: examining the causality. *Nat. Rev. Gastroenterol.* **18**, 3–4 (2021).
5. Steenblock, C. et al. Viral infiltration of pancreatic islets in patients with COVID-19. *Nat. Commun.* **12**, 3534 (2021).
6. Müller, J. A. et al. SARS-CoV-2 infects and replicates in cells of the human endocrine and exocrine pancreas. *Nat. Metab.* **3**, 149–165 (2021).
7. van der Heide, V. et al. Limited extent and consequences of pancreatic SARS-CoV-2 infection. *Cell Rep.* **38**, 110508 (2022).
8. Kusmartseva, I. et al. Expression of SARS-CoV-2 entry factors in the pancreas of normal organ donors and individuals with COVID-19. *Cell Metab.* **32**, 1041–1051.e6 (2020).
9. Sjöstedt E., et al. An atlas of the protein-coding genes in the human, pig, and mouse brain. *Science* **367** (2020).
10. Mao, M. et al. Multifaced roles of PLAC8 in cancer. *Biomark. Res.* **9**, 73 (2021).
11. Kaistha, B. P. et al. PLAC8 localizes to the inner plasma membrane of pancreatic cancer cells and regulates cell growth and disease progression through critical cell-cycle regulatory pathways. *Cancer Res.* **76**, 96–107 (2016).
12. Kinsey, C. et al. Plac8 links oncogenic mutations to regulation of autophagy and is critical to pancreatic cancer progression. *Cell Rep.* **7**, 1143–1155 (2014).
13. Tatura, M. et al. Placenta-specific 8 is overexpressed and regulates cell proliferation in low-grade human pancreatic neuroendocrine tumors. *Neuroendocrinology* **110**, 23–34 (2020).
14. Ugalde, A. P. et al. Autophagy-linked plasma and lysosomal membrane protein PLAC8 is a key host factor for SARS-CoV-$_2$ entry into human cells. *EMBO J.* **41**, e110727 (2022).
15. Tse, L. V. et al. Genomewide CRISPR knockout screen identified PLAC8 as an essential factor for SADS-CoVs infection. *Proc. Natl Acad. Sci.* **119**, e2118126119 (2022).
16. Torrens-Mas, M. et al. GDF15 and ACE2 stratify COVID-19 patients according to severity while ACE2 mutations increase infection susceptibility. *Front Cell Infect. Microbiol.* **12**, 942951 (2022).
17. Díez, J. M. et al. Cross-neutralization activity against SARS-CoV-2 is present in currently available intravenous immunoglobulins. *Immunotherapy* **12**, 1247–1255 (2020).
18. Saiz, M. L. et al. Epigenetic targeting of the ACE2 and NRP1 viral receptors limits SARS-CoV-2 infectivity. *Clin. Epigenet.* **13**, 187 (2021).
19. Byeon, S. K. et al. Development of a multiomics model for identification of predictive biomarkers for COVID-19 severity: a retrospective cohort study. *Lancet Digit. Heal* **4**, e632–e645 (2022).
20. Bankhead, P. et al. QuPath: Open source software for digital pathology image analysis. *Sci. Rep.* **7**, 16878 (2017).
21. Burgess, S. et al. Guidelines for performing Mendelian randomization investigations. *Wellcome Open Res.* **4**, 186 (2019).
22. Ferkingstad, E. et al. Large-scale integration of the plasma proteome with genetics and disease. *Nat. Genet.* **53**, 1712–1721 (2021).
23. Prasad, H. et al. COVID-19 and serum amylase and lipase levels. *Indian J. Surg.* **85**, 337–340 (2023).
24. Batra, H. et al. Comparative study of serum amylase and lipase in acute pancreatitis patients. *Indian J. Clin. Biochem* **30**, 230–233 (2015).
25. Gomez, D. et al. Retrospective study of patients with acute pancreatitis: is serum amylase still required? *BMJ Open* **2**, e001471 (2012).
26. Ismail, O. Z. & Bhayana, V. Lipase or amylase for the diagnosis of acute pancreatitis? *Clin. Biochem.* **50**, 1275–1280 (2017).
27. Wang, F. et al. Pancreatic injury patterns in patients with coronavirus disease 19 pneumonia. *Gastroenterology* **159**, 367–370 (2020).
28. Initiative C-19 HG, Leadership, Pathak, G. A. et al. A first update on mapping the human genetic architecture of COVID-19. *Nature* **608**, E1–E10 (2022).
29. McCluskey, J. T. et al. Development and functional characterization of insulin-releasing human pancreatic beta cell lines produced by electrofusion. *J. Biol. Chem.* **286**, 21982–21992 (2011).
30. Beumer, J. et al. A CRISPR/Cas9 genetically engineered organoid biobank reveals essential host factors for coronaviruses. *Nat. Commun.* **12**, 5498 (2021).
31. Qadir, M. M. F. et al. SARS-CoV-2 infection of the pancreas promotes thrombo-fibrosis and is associated with new-onset diabetes. *JCI Insight* **6**, e151551 (2021).
32. Yang, J.-K. et al. Binding of SARS coronavirus to its receptor damages islets and causes acute diabetes. *Acta Diabetol.* **47**, 193–199 (2010).
33. Ding, Y. et al. Organ distribution of severe acute respiratory syndrome (SARS) associated coronavirus (SARS-CoV) in SARS patients:

implications for pathogenesis and virus transmission pathways. *J. Pathol.* **203**, 622–630 (2004).
34. Wang, Y. et al. Kinetics of viral load and antibody response in relation to COVID-19 severity. *J. Clin. Invest.* **130**, 5235–5244 (2020).
35. Chua, R. L. et al. COVID-19 severity correlates with airway epithelium–immune cell interactions identified by single-cell analysis. *Nat. Biotechnol.* **38**, 970–979 (2020).
36. Wauters, E. et al. Discriminating mild from critical COVID-19 by innate and adaptive immune single-cell profiling of bronchoalveolar lavages. *Cell Res.* **31**, 272–290 (2021).
37. Schneider, C. A., Rasband, W. S. & Eliceiri, K. W. NIH Image to ImageJ: 25 years of image analysis. *Nat. Methods* **9**, 671–675 (2012).
38. Scharfmann, R. et al. Mass production of functional human pancreatic β-cells: why and how? *Erratum: Diab. Obes. Metab.* **18**, 1288 (2016).

Acknowledgements

We thank Prof Carlos López Otín for the helpful comments. We thank Pau Pericàs-Pulido from PRISIB for technical assistance. We thank Dr. Catalina Perello-Reus for the helpful comments and assistance. We thank Victoria E Cano-Garcia from IDISBA Biobank for her assistance with sample processing. We are grateful to Dr. Thomas Peackock for kindly providing SARS-CoV-2 Spike plasmids. We thank Luis Enjuanes, at CNB-CSIC, for providing us with Vero E6 cells and the Wuhan-1, and BA.1 strains of SARSCoV-2. We thank Dr. Marcos Malumbres (CNIO) for providing HPAF-II MIA PaCa-2 and SUIT-2 cell lines. We thank Dr Alexander Kleger for providing a 1.4E7 cell line (Ulm University, Germany). We thank Uta Lehnert, Juliane Nell, and Ralf Köhntop for technical assistance. The imaging facility at the CMCB Technology Platform at TU Dresden is thanked for its assistance with imaging. The German Registry for COVID19 Autopsies (DeRegCovid) is thanked for giving us access to the tissues from Regensburg. This work was funded by the Instituto de Salud Carlos III (ISCIII) and Programa de Investigación en Salut—ISCIII (PI20/01267), by Fondo COVID19-ISCIII (COV20/00571), by Fundació La Marató (MARATÓ 167-C-2021 51), co-funded by the European Union and through the Programa Miguel Servet (MS19/00100) co-funded by the European Regional Development Fund/European Social Fund, "A way to make Europe"/"Investing in your future" (CB); TECH fellowship program, Impost turisme sostenible/Govern de les Illes Balears (TECH19/03) (LI-G). Ministerio de Ciencia e Innovación MCIN/AEI /10.13039/501100011033 / FEDER, UE (PID-2021-123810OB-I00) and the European Commission – NextGenerationEU (Regulation EU 2020/2094), by Ministerio de Ciencia e Innovación MCIN/AEI /10.13039/501100011033/ European Union NextGenerationEU/PRTR (CNS2022- 135276) (MLD); and through Spanish National. Research Council (CSIC)'s Global Health Platform (PTI Salud Global, CSIC-COV19-012/012202020E086) (MLD); ". The project that gave rise to these results received the support of a fellowship from "la Caixa" Foundation (ID 100010434). The fellowship code is LCF/BQ/DR22/11950020, awarded to DLG (DLG); Ministerio de Ciencia e Innovación (RYC2021-031776-I) (APU), the Deutsche Forschungsgemeinschaft (DFG, German Research Foundation) project numbers 314061271 and 288034826 (CS). SH is supported by Ulm University Hertha Nathorff and Medical Scientist Program funding. The funding bodies did not play any role in study design, data collection, data analyses, interpretation, or writing of the report.

Author contributions

Conducted experiments: L.I.-G., S.H., M.L.-D., D.L.-G., P.G., S.A.-P., C.C., J.A.M.-G., C.S., H.D. Investigation: C.C., E.C.-B., A.P.U., G.B., M.L..D., C. Designed experiments: S.H., M.L.-D., T.F.E.B., I.F.-C., C.S., C.B. Provided funding: C.S., A.K., C.B., M.L.-D. Writing, reviewing and editing: S.H., M.L.-D., T.F.E.B., I.F.-C., C.S., C.B.

Competing interests

The authors declare no competing interests.

Additional information

Supplementary information The online version contains supplementary material available at https://doi.org/10.1038/s43856-025-00745-6.

Correspondence and requests for materials should be addressed to Marta L. DeDiego or Carles Barceló.

Peer review information *Communications Medicine* thanks the anonymous reviewers for their contribution to the peer review of this work. A peer review file is available.

Reprints and permissions information is available at http://www.nature.com/reprints

Publisher's note Springer Nature remains neutral with regard to jurisdictional claims in published maps and institutional affiliations.

[1]Translational Pancreatic Cancer Oncogenesis Group, Health Research Institute of the Balearic Islands (IdISBa), Hospital Universitari Son Espases, Palma de Mallorca, Spain. [2]Institute of Molecular Oncology and Stem Cell Biology, Ulm, Germany. [3]Department of Molecular and Cell Biology, Centro Nacional de Biotecnología (CNB-CSIC), Madrid, Spain. [4]Department of Pathology, Ulm University Hospital, Ulm, Germany. [5]Hospital Universitari Son Espases, Palma de Mallorca, Spain. [6]Stroke Pharmacogenomics and Genetics Group, Sant Pau Biomedical Research Institute, Barcelona, Spain. [7]Health Research Institute of the Balearic Islands (IdISBa), Palma de Mallorca, Spain. [8]Internal Medicine Department, Son Llàtzer University Hospital, Palma de Mallorca, Spain. [9]Departamento de Bioquímica y Biología Molecular, Instituto Universitario de Oncología (IUOPA), Universidad de Oviedo, Oviedo, Spain. [10]Department of Internal Medicine III, University Hospital Carl Gustav Carus, Technische Universität Dresden, Dresden, Germany. [11]Division of Interdisciplinary Pancreatology, Department of Internal Medicine I, Ulm University Hospital, Ulm, Germany. [12]Faculty of Health Sciences, Universitat Oberta de Catalunya, Barcelona, Spain. [13]Present address: Faculty of Health Sciences at Manresa, Universitat de Vic—Universitat Central de Catalunya (UVic-UCC), Barcelona, Spain. [14]These authors contributed equally: Lesly Ibargüen-González, Sandra Heller.
✉e-mail: marta.lopez@cnb.csic.es; carles.barcelo@gmail.com; CBarcelo@umanresa.cat